ACS OMEGA

http://pubs.acs.org/journal/acsodf Article

Impact of Growth Temperature of Lead-Oxide Nanostructures on the Attenuation of Gamma Radiation

Raghad Y. Mohammed, Furman Kasseem Ahmed, Ahmed Fattah Abdulrahman,* Samir Mustafa Hamad, Sabah M. Ahmed, Azeez Abdullah Barzinjy, and Munirah Abdullah Almessiere

Cite This: *ACS Omega* 2023, 8, 22230−22237 Read Online

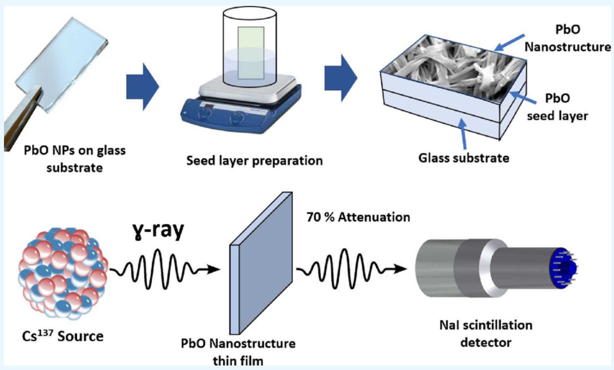

ABSTRACT: Chemical bath deposition (CBD) technique is utilized to grow lead-oxide (PbO) nanostructures (NSs) over PbO seed fabricated by physical vapor deposition (PVD) method on glass substrates. The effect of growth temperatures 50 and 70 °C on the surface topography, optical properties, and crystal structure of lead-oxide NSs has been studied. The investigated results suggested that the growth temperature has a huge and very considerable influence on the PbO NS, and the fabricated PbO NS has been indexed as the Pb_3O_4 polycrystalline tetragonal phase. The crystal size for PbO thin films grown at 50 °C was 85.688 nm and increased to 96.61 nm once the growth temperature reached 70 °C. The fabricated PbO nanofilms show a high rate of transmittance, which are ∼70 and 75% in the visible spectrum for the films deposited at 50 and 70 °C, respectively. The obtained E_g was in the range of 2.099−2.288 eV. Also, the linear attenuation coefficient values of gamma-rays for shielding the Cs-137 radioactive source increased at 50 °C. The transmission factor, mean free path, and half-value layer are reduced at a higher attenuation coefficient of PbO grown at 50 °C. This study evaluates the relationship between synthesized lead-oxide NSs and the radiation energy attenuation of gamma-rays. This study provided a suitable, novel, and flexible protective shield of clothes or an apron made of lead or lead oxide to protect against ionizing radiation that meets safety rules and protects medical workers from ionizing radiation.

1. INTRODUCTION

Ionizing radiation has been used since the beginning of the twentieth century. There are many detailed studies on its outward effects on the population exposed to radiation from atomic bombs and on health workers such as radiologists and patients who have been exposed to radiotherapy, and this effect represents cancer.[1] Exposure to ionizing radiation continuously affects living cells, causing disease and even death. Therefore, providing safety conditions should be considered for people exposed to this radiation daily for various purposes.[2,3] Three basic routines are used to minimize the exterior radiation risks such as time, distance, and shielding. Radiation shielding (gamma-ray and X-ray) is considered one of the most important things necessary for radiation workers and the general public.[4,5] Gamma-ray and X-ray attenuation coefficients are very significant in numerous practical fields, such as nuclear diagnostics, radiation dosimetry, radiation protection (RP), and nuclear medicine.[6] Lead (Pb, Z 1/4 82) is the most common RP material because it has a high value of mass number in order to attenuate gamma radiation and provides the best shield against gamma radiation used in medical, industrial, and nuclear reactors.[7] Nowadays, there are more requests for the use of novel compounds for RP (attenuator). One of the most common RP materials is nanostructures (NSs). NSs have become a big deal because of their unique optical, electrical, magnetic, thermal, and chemical properties. Metal oxides are the most significant NSs due to their implementation in various technologies and devices. These technologies, which include optoelectronic devices, solar cells, and batteries with great pursuit and stability at high anodic potentials, are significant in their use for the electrochemical construction of different synthetic substances utilized in chemical work and for the change of unsafe poisons into less harmful accumulates by electrochemical strategies.[8−10] Among these metal oxides, lead oxide (PbO) has the most significant use in depot batteries, glass business, and dyes.[11] Till now, different shapes of PbO NSs have been fabricated, for instance,

Received: April 27, 2023
Accepted: May 26, 2023
Published: June 8, 2023

https://doi.org/10.1021/acsomega.3c02910
ACS Omega 2023, 8, 22230−22237

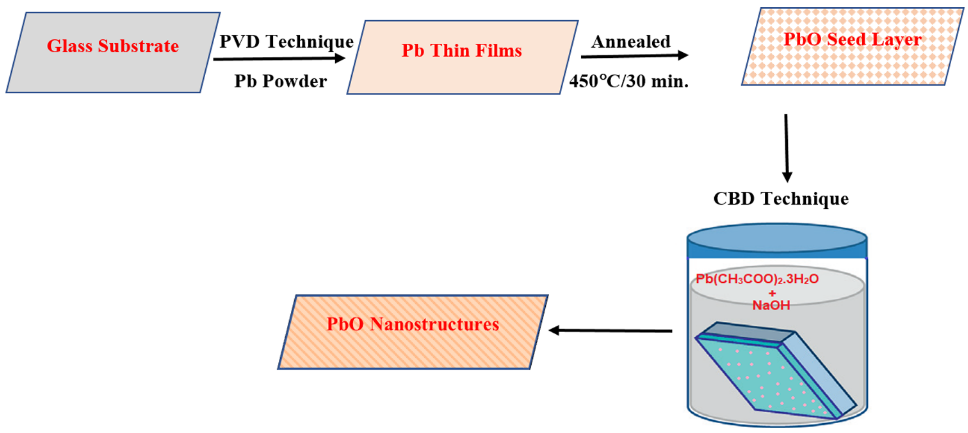

Figure 1. Schematic diagram of the growth of PbO NSs.

nanoplates, nanostars,[12] nanorods,[13] nanopowders,[14,15] nanosheets, and nanotubes.[16] However, PbO is a vital semiconductor compound that exhibits excellent potentials: small electrical conductivity, broad band gap, great photoconductivity, and fascinating chemical and thermal steadiness.[17−19]

Lead-oxide nanoparticles can be toxic if they are not handled and used properly. Lead is a toxic heavy metal, and when it is breathed in or swallowed in high concentrations, it can cause serious health problems. Exposure to lead-oxide nanoparticles has been demonstrated to be harmful to the nervous system, kidneys, and liver. Hence, it is crucial to exercise caution when working with lead-oxide nanoparticles and adhere to all necessary safety protocols.[11]

PbO can be classified into two types, α-PbO and β-PbO, based on their band gaps with energies of 1.92 and 2.7 eV, respectively, which are attributed to their unique mechanical, electrical, and optical characteristics.[17,18,20] Therefore, lead monoxide is effective for protecting from radioactivity owing to its high density (9.53 g/cm^3).[21] Also, PbO has a yellow color and a high-atomic-number concentration. Moreover, it is a favorable compound appropriate for low-dose, high-resolution imaging. Lead oxide can be formed in different structure phases, such as PbO (α,β), Pb_2O_3, Pb_3O_4, and PbO_2 (α,β).[20,22] It is worthy to mention that PbO is being used to improve the glass's resistance to diversity, reduce the melting temperature, and enhance the chemical strength of the material. As mentioned in a previous work, there are many ways to create both bulk PbO and nanopowder PbO, but attempting to find a simple way to make PbO with control over its size and shape is still being looked for. Currently, there are several approaches or techniques, such as chemical, physical, and biological approaches, to fabricate PbO NSs.

Among these methods for the synthesis of PbO, the chemical bath deposition (CBD) technique, which is more affordable than other deposition methods, is considered for the production of moderately easy gadgets, particularly light detectors and light energy conversion cells. A few endeavors stood to obtain binary metal oxides utilizing the CBD technique[23,24] for effective solar energy conversion through photo-electrochemical solar cells.

The structure of a material plays a significant role in determining its ability to shield gamma radiation. The shielding properties of a material depend on the combination of its atomic number, composition, density, and structural properties. Different structures have different atomic numbers and composition of materials which can significantly affect its radiation shielding properties. Generally, materials with higher atomic numbers, such as lead or tungsten, are more effective at blocking gamma radiation due to their greater capacity for absorbing and scattering photons.[25] Tekin et al. studied the microstructures and NSs of a material that have an impact on its radiation shielding qualities. For example, materials with a fine-grained micro- or nanostructure may be more effective at blocking gamma radiation due to an increase in the number of interfaces and grain size available for photon absorbing.[26] Pomaro investigated a material's crystalline structure effect and its ability to block gamma radiation. He showed that gamma radiation can be scattered more efficiently by crystalline and more ordered materials, as opposed to amorphous materials.[27] Moreover, the higher growth rate or thickness plays a crucial role in determining its gamma radiation shielding characteristics. Although thicker materials provide more options for photon scattering and absorption, they are typically more effective in preventing gamma radiation.[28] Kim studied the material structures that have different voids or particle size arrangements, which when blended with a polymer material can affect its radiation shielding performance. It was revealed that the clustering and shielding effects in the high-energy region increased with the particle size. As a result, the shielding effectiveness can be raised. The impact of particle size on the shielding effectiveness was minimal in the low-dose area.[29]

In this work, the CBD process was used to produce PbO NSs on glass substrates in order to provide a flexible protective shield of fabric or an apron made of lead or lead-oxide material. The PbO NSs are used for protection against ionizing radiation to meet safety requirements and protect medical people from ionizing radiation. The effects of the growth temperatures on the surface morphology, optical properties, and crystal structure of PbO NSs have been investigated. Besides, the relationship between the growth temperature of lead-oxide NSs and gamma-ray attenuation has been evaluated.

2. EXPERIMENTAL DETAILS

In the current study, all chemicals used, which include lead acetate [$Pb(C_2H_3O_2)_2 \cdot 3H_2O$], and sodium hydroxide (NaOH) were ordered from Sigma-Aldrich without further purification. Double-distilled water (DDW) has been employed for production and treatment (cleaning) processes. Generally, the growth of the PbO seed layer is very significant for the growth of final nanostructural materials. PbO thin film can be used as a nucleation seeds layer for the synthesis of PbO

https://doi.org/10.1021/acsomega.3c02910
ACS Omega 2023, 8, 22230−22237

NSs.[30] First, glass slides (25 × 75 × 1 mm^3) were used to deposit PbO thin film as a seed layer. Washing and cleaning of glass slides are the main processes that affect the properties of the seed layer and NS.[24] First, the glass (PbO seed layer) substrates were dipped for 24 h at room temperature (RT) in a container filled with chromic acid. After that, the prepared samples or substrates were cleaned with DDW for 15 min using an ultrasonic bath, and after that, they were immersed or dipped in acetone for 15 min and rinsed again with DDW. Finally, the substrates were dried in air at room temperature and kept in a desiccator.[31] This cleaning process provides a better nucleation center for growth, good adhesion, and uniform deposition of the final structure.[15]

Second, the seed layer of PbO was synthesized employing the physical vapor deposition (PVD) technique, following the same procedure explained by Ahmed et al. and Nwodo et al.[15,32] Then, PbO NSs were produced and grown on the seed layer through the use of CBD synthesis. 0.1 M $Pb(C_2H_3O_2)_2 \cdot 3H_2O$ aqueous solution was prepared using DDW, and 1.9 M NaOH was added to the mixture in a beaker to control the pH value of the reaction solution and stirred vigorously and then set at 50 and 70 °C. The substrates were then taken out after 10 min. The produced PbO NS samples were cleaned very well with DDW many times and ultrasonic bath agitation to remove or decrease the porosity of the NSs of PbO over the layer, and then the samples were dried in air at RT and evacuated or stored in a desiccator container. All the samples were prepared at pH = 13.5. A schematic diagram for the production and growth of PbO NS samples is shown in Figure 1

An optical interferometer analysis technique was employed to estimate the PbO thin-film thickness.[33] The crystal structure properties of the PbO samples were obtained and studied by employing an X-Pert Pro Analytical X-ray diffraction machine with an XRD scanning range of 2θ set from 20° to 70°, a wavelength of 1.5406 Å from $Cu_{K\alpha}$ operating voltage at 40 kV, and current at 30 mA. A double-beam UV−visible spectrophotometer in the wavelength range of 400−1100 nm was used to scan the transmittance spectra of the PbO thin films.

The NaI scintillation detector was employed to record and examine the efficiency of PbO NSs (grown on a glass substrate at both deposition temperatures of 50 and 70 °C) to attenuate the gamma-ray emitted by the radioactive source cesium-137 (Cs-137). The intensity measured for the gamma-rays traveling through the fabricated lead oxide NSs was given as a function of temperature. To find more accurate results regarding the optimum degree of deposition for PbO NSs, we used a variety of equations related to the attenuation of gamma-ray radiation, such as the linear attenuation coefficients (μ), the half-value layer (HVL), the radiation attenuation ratios (RARs), the mean free path (MFP), and the transmission coefficient (TF), as shown in Figure 2.

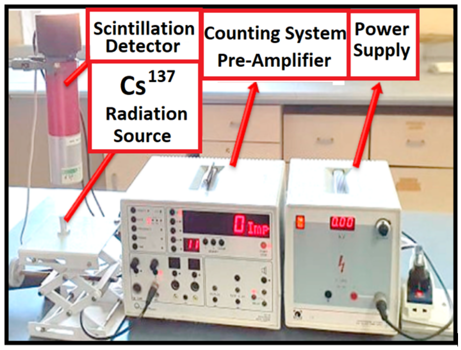

Figure 2. Experimental setup of testing and examining the synthesized PbO NS thin-film samples as the gamma radiation attenuation.

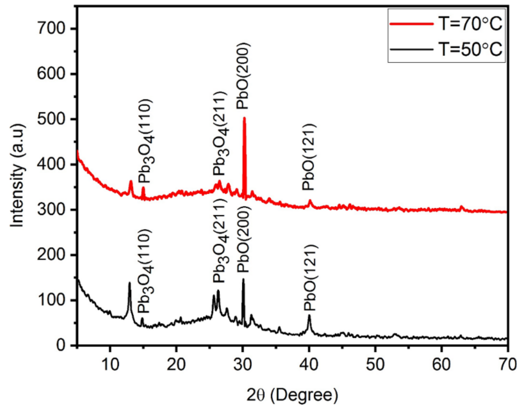

Figure 3. XRD patterns of the produced PbO NSs by using the CBD method at different deposition temperatures.

3. RESULTS AND DISCUSSION

3.1. Crystal Structure Properties of Lead-Oxide NSs. The XRD patterns of the produced PbO NS thin films by using the CBD method at different deposition temperatures of 50 and 70 °C are shown in Figure 3. All investigated peaks of diffraction at all temperatures were indexed as a polycrystalline PbO and Pb_3O_4 tetragonal crystal structures, which correspond to and are matched to the standard XRD database spectra of the PbO NSs (CPDS card nos 2791, 2921, and 2923).

In addition, other imperfection (defect) peaks were not obtained, indicating that the high purity PbO nanocrystal was grown. Besides, the strongest diffraction peaks of PbO NSs at 2θ = 30.215° and 40.095° are conformable to the two planes (200) and (121), respectively. The sharpness and high intensity of the diffraction peaks afford an indication of the very high polycrystalline quality of the PbO material produced.[34] The obtained XRD patterns in the current work are in good correspondence with previous studies.[34] The characteristics of the crystal structure of the PbO NSs, such as the crystal size (D), the dislocation density (δ), the peak position (2θ), and the full width at half-maximum (FWHM) of the produced PbO samples at different temperatures 50 and 70 °C alongside the stronger diffraction peaks, are listed and summarized in Table 1.

The crystal size of the PbO NSs synthesized at 70 °C is bigger than that synthesized at 50 °C as shown in Table 1. This difference in the crystal size may be due to the various values of the FWHM, imperfections, and internal stress because there is a lattice mismatch between PbO NSs and glass-slide substrates. The bigger size of PbO crystallites may be attributed to the larger value of unit cell volume, which is consistent with previous work.[35−39]

3.2. Morphological Characteristics of Lead-Oxide NSs. The surface morphology (top view) of the produced PbO NSs at several deposition temperatures (50 and 70 °C) are shown in Figure 4. At a deposition temperature of 50 °C, the nanofiber like PbO NSs were produced on the PbO seed layer (Figure 4a). While increasing the growth temperature to 70 °C, the nanoflowers like PbO NSs over the nanoseed layer

https://doi.org/10.1021/acsomega.3c02910
ACS Omega 2023, 8, 22230−22237

Table 1. Lead Oxide NS Crystal Structure Characteristics

growth temperature (°C)	(hkl)	FWHM	2θ	D (nm)	δ (Å) $\times 10^{-6}$	d_{hkl}
50	200	0.096	30.081	85.688	1.3619	2.9683
70	200	0.086	30.256	95.691	1.09207	2.9516

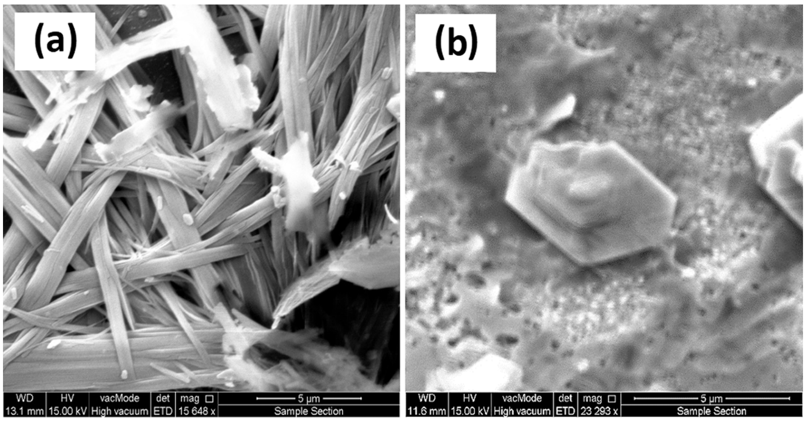

Figure 4. Surface morphology top-view FESEM image of the PbO nanostructure synthesis at 10 min for different growth temperatures. (a) 50 °C and (b) 70 °C.

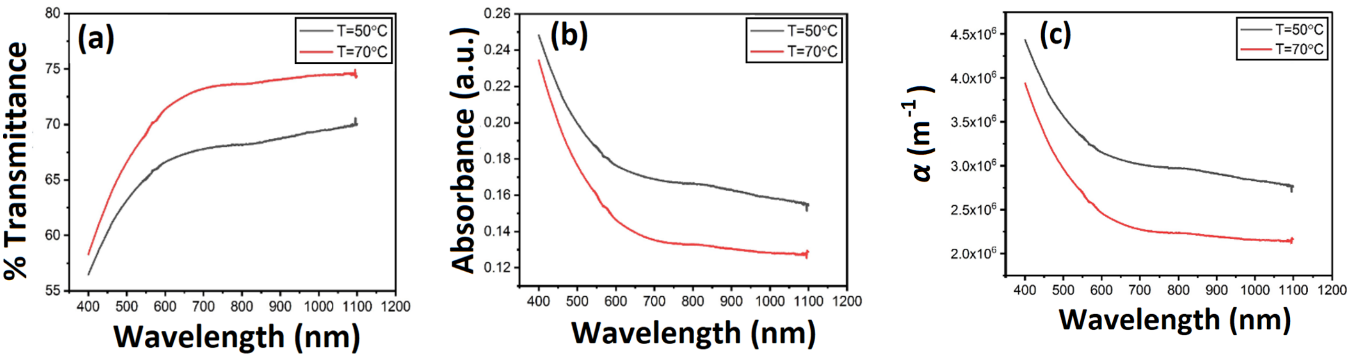

Figure 5. (a) Optical transmittance spectra, (b) optical absorbance spectra, and (c) absorption coefficient of the produced PbO NSs at several deposition temperatures.

were developed (Figure 4b). It can be noticed that the growth (reaction) temperature has a very significant impact on the lead-oxide structure.

The morphology of NSs can be significantly affected by the growing temperature, which is a crucial parameter. It is possible to precisely regulate the temperature during the growing process to adjust the NS's size and shape to suit certain needs. At different growth temperatures, the crystal structure of the NS may change, which can affect the overall morphology, for example, at higher temperatures, some materials may transition from a crystalline to amorphous phase. In addition, the growth rate of NSs can vary significantly with growth temperature. At higher growth temperatures, the growth rate could be increased, leading to more complex NSs; this is because the mobility of atoms and molecules on the surface of the NS can be influenced by the temperature which in turn can affect the shape of the structure and would be a more compact structure.[40]

3.3. Optical Properties of Lead-Oxide NSs. The optical properties of the fabricated NS are important; they depend on the energy of the incident photon, thickness, crystal structure, morphology, and chemical composition of the growth material. The results of transmittance, absorbance, and absorption coefficient are shown in Figure 5.

From Figure 5a, one can demonstrate that the films have a high rate of transmittance (~70 and 75%) in the visible spectrum for the films grown at 50 and 70 °C, respectively. The high transmittance materials are important for antireflection deposition on transparent covers or windows of solar thermal devices to decrease the reflectance, increase the rate of transmittance, and enhance their efficiencies.[33] The absorption spectra and absorption coefficient (Figure 5b,c) are the simplest techniques (methods) for probing the optical properties of semiconductors.[41] In addition, the energy band gap of the deposited NSs was estimated by using Tauc's plot equation to evaluate the direct band gap energy of the NS as follows:

$$\alpha = (h\nu - E_g)^2 \quad (1)$$

where α is the thin-film absorption coefficient, hν is the incident photon energy, and E_g is the band gap energy;[41] plot $(\alpha h\nu)^2$ versus $h\nu$ is shown in Figure 6.

The calculated values of band gap energy for grown PbO at 50 °C is 2.099 eV, and it increased to 2.288 eV for PbO grown at 70 °C. The estimated values of E_g are in good agreement with previous published studies.[42] The E_g is correlated with the stress state, carrier concentration, and grain size of the

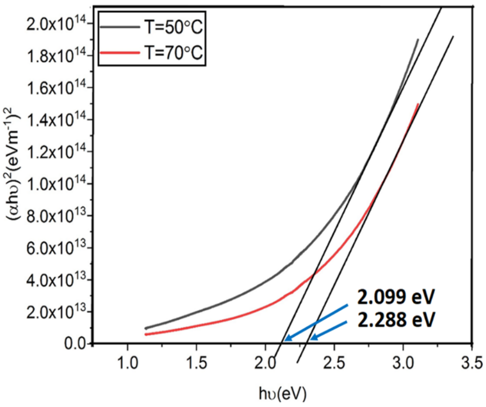

Figure 6. $(\alpha h\nu)^2$ versus $h\nu$ for PbO thin films grown at 50 and 70 °C, respectively.

materials. Besides, the broadening of the energy band gap values with growth (reaction) temperatures up to 70 °C is possibly due to the enhancement of the transition tail width as a result of a higher rate of the compressive strain along the (200) plane.

3.4. Gamma-Ray Attenuation Measurements. Gamma radiation loss takes place either by the photoelectric effect (the photon completely disappears) or partially by the Compton effect (the photon transfers a portion of its energy to the electron), depending on the amount of initial energy. Gamma radiation is attenuated exponentially when it passes through any material.[43] The relation between the gamma-ray emitted from Cs-137 and the shielding material PbO NSs was calculated by the following equation:[44]

$$C = C_o e^{-\mu x} \tag{2}$$

Here, C is the intensity of the attenuated gamma-ray, C_o is the initial intensity, x (cm^{-1}) is the thickness of the shielding material, and μ (1/cm) is the attenuation coefficient of the shielding PbO NSs. The linear attenuation coefficient is related to incident gamma-ray energy, shielding material, and material density. Materials used in different structures have different densities. There is certain probability that radiation will interact with the atoms of the shielding materials when it passes through various shielding structures. This causes different amounts of radiation energy to be absorbed.

Also, density is the main factor that affects the shielding properties because higher densities have more atomic number, which increases the amount of radiation that can be absorbed and scattered. However, there are other factors that can also affect the shielding properties, including thickness, composition, distance from the source, exposure time, angle of incidence, and others. The effect of the shielding material PbO NSs on the average rate of the radiation attenuation at both deposition temperatures 50 and 70 °C is summarized in Table 2.

According to the obtained results (Table 2), the nanolayered samples that were coated with PbO NSs using the CBD technique at 50 °C had preferable shielding efficiency or abilities when compared to those that were deposited at 70 °C. The attenuation coefficients (μ) of PbO NSs decrease with increasing deposition temperature at 70 °C. This coefficient was used to calculate the HVL, which is the thickness of the shield or absorbent material that decreases the level of the radiation by a factor of 2 to half (1/2) of the initial level.[45]

$$\text{HVL} = \frac{\ln 2}{\mu} \tag{3}$$

The HVL was estimated in this study to analyze the penetrating ability of gamma radiation through PbO NSs grown on a glass layer under different temperatures 50 and 70 °C, and it reduces with an increase of μ. As shown in Table 2, the lead-oxide NSs have highly efficient rate of performance for protection from the radiation, and the obtained results are better than those from previous studies.[46,47]

The SEM images in Figure 4 revealed that the PbO sample grown at 50 °C has a more and clear grain boundary structure compared to the PbO sample synthesized at 70 °C. In addition, the crystal quality of 50 °C samples is higher than the other one; see Figure 3. These results prove that the radiation shielding capacity and the gamma-ray absorption were achieved more by the optimized sample grown at 50 °C.

The MFP is defined as the average distance a photon travels between two collisions with atoms of the target material. It is a significant parameter in designing the radiation shielding material, and it depends on the type of material and the energy of the photon. The MFP is represented by the following equation:[43]

$$\text{MFP} = \frac{1}{\mu} \tag{4}$$

High-density materials provide more significant interaction potential for photons and better shielding properties. Table 2 shows that at higher growth temperature of 70 °C, the density of the PbO NSs decreases and the crystal size of nanoparticles increases, which have an effect on the interaction potential of photons. This, in turn, reduces the value of the attenuation coefficient. Therefore, shielding materials that have lower HVL and MFP values are preferred for shielding purposes. The shield performances of the RARs of PbO NSs at 50 and 70 °C deposition temperatures are calculated by the following equation:

$$\text{RAR}\ (\%) = \left[\frac{C_o - C}{C_o}\right] \times 100 \tag{5}$$

Table 2. Average Rate of the Radiation Attenuation Was Measured Based on PbO NS Thin Films Produced at Several Deposition Temperatures

deposition temperature (°C)	average rate of radiation attenuation (coun./s)	thin-film thickness (m)	μ (cm^{-1})	HVL (cm)	MFP (cm)	attenuation rate %	$T(E,x)$
0	48.6417	0				0	
(50)	14.5917	1.29×10^{-7}	9333333.33	7.4250×10^{-8}	1.071×10^{-7}	70.0017	0.2999
(70)	30.8333	1.37×10^{-7}	3324817.52	2.0847×10^{-7}	3.007×10^{-7}	36.6112	0.6338

https://doi.org/10.1021/acsomega.3c02910
ACS Omega 2023, 8, 22230−22237

At 50 °C of growth temperature, the shield of PbO NSs shows better performance on the RAR, as shown in Table 2.

The other factor used to perform shielding calculations is theTF. The TF of any matter, $T(E,x)$ for gamma-ray energy (E) through the thickness x (cm) of shield material, is defined by dividing the gamma-ray intensity $C(E,x)$ or C of the shielding material with thickness x by the gamma-ray intensity in the absence of the shielding material $C_o(E,0)$ or C_o, as shown in the following equations:[48,49]

$$T(E,\, x) = \frac{C(E,\, x)}{C_o(E,\, o)} \tag{6}$$

The TF increases by increasing the shield deposition temperature at 70 °C, so the behavior of the TF and the linear radiation attenuation coefficient (μ) are varied because the relationship between them is inverse. In Table 2, PbO nanostructurs produced over the substrate at a reaction (deposition) temperature of 50 °C showed a higher impedance to transmit gamma radiation. The measured HVL thickness of PbO was much less than that of ordinary lead. Therefore, PbO NSs have a high efficiency to attenuate gamma (γ) radiation and act as shields against the source of γ radiation, and the obtained results of HVL are better than those from the previous studies.[47]

The growth temperature of a material during synthesis affects its morphology and crystal structure. The growth temperature influences atoms and molecules mobility in the growth environment, which affects the rate of nucleation, growth, and diffusion. Material morphology refers to its shape, size, and surface properties. Morphology can affect the scattering and absorption of radiation shielding. For example, rough surfaces scatter and absorb radiation better than smooth ones. The material thickness and shape also affect RP. Material radiation shielding depends on its crystal structure and chemical composition. High-density, high-atomic-number materials can attenuate high-energy radiation. Density of nanoparticles, crystal size, grain size, and defect structure are affected by the material's crystal structure and orientation, which improve radiation shielding. Absorption and scattering photons increase radiation shielding. The growth temperature affects a material's morphology, crystal quality, and chemical composition, which are in turn influenced by the growth temperature. Therefore, optimizing the growth temperature produces better material for RP.[50−52]

4. CONCLUSIONS

The CBD technique was used to successfully deposit high-quality PbO NSs. The PbO seed layer was deposited on the glass substrate by employing the PVD technique. The impact of the growth temperatures on the topography, the structural characteristics, and the optical properties was estimated. The obtained results suggested that the growth temperature has a huge and very considerable influence on the PbO NS, and it is indexed as the Pb_3O_4 polycrystalline tetragonal phase. The crystal size for thin films grown at 50 °C was 85.688 nm and increased to 96.61 nm soon after the growth temperature reached 70 °C. The produced PbO NSs show high transmittance (~70 and 75%) in the visible spectrum for the films deposited at 50 and 70 °C, respectively. The energy band gap for PbO grown at 50 °C is 2.099 eV, and it increased to 2.288 eV for PbO grown at 70 °C. According to this study, the linear attenuation coefficient values of gamma-rays for shielding a Cs-137 radioactive source increased at 50 °C. TF, MFP, and HVL are reduced at a higher attenuation coefficient of PbO grown at 50 °C. Fabricated PbO NSs showed significant radiation shielding performance in radiation attenuation. The results obtained from this investigation could have uses in possible applications for gamma shielding materials. There is a new way to protect people from radiation. Synthetic PbO nanomaterials can protect against gamma-rays because of their fixable and small thickness. It can be used for fabricating clothing out of lightweight materials and are useful as potential gamma-ray and X-ray shielding materials.

AUTHOR INFORMATION

Corresponding Author

Ahmed Fattah Abdulrahman − *Department of Physics, Faculty of Science, University of Zakho, 42002 Zakho, Kurdistan Region, Iraq; Department of Computer and Communications Engineering, College of Engineering, Nawroz University, 42001 Duhok, Kurdistan Region, Iraq;* orcid.org/0000-0002-1762-5029; Email: ahmed.abdulrahman@uoz.edu.krd

Authors

Raghad Y. Mohammed − *Department of Physics, College of Science, University of Duhok, 42001 Duhok, Kurdistan Region, Iraq*

Furman Kasseem Ahmed − *Physiotherapy Department, Hawler Medical University/College of Health Science, 44001 Erbil, Kurdistan Region, Iraq*

Samir Mustafa Hamad − *Scientific Research Center, Soran University, 44008 Erbil, Iraq*

Sabah M. Ahmed − *Department of Physics, College of Science, University of Duhok, 42001 Duhok, Kurdistan Region, Iraq*

Azeez Abdullah Barzinjy − *Scientific Research Center, Soran University, 44008 Erbil, Iraq;* orcid.org/0000-0003-4009-9845

Munirah Abdullah Almessiere − *Department of Physics, College of Science and Department of Biophysics, Institute for Research and Medical Consultation (IRMC), Imam Abdulrahman Bin Faisal University, 31441 Dammam, Saudi Arabia;* orcid.org/0000-0003-1651-3591

Complete contact information is available at: https://pubs.acs.org/10.1021/acsomega.3c02910

Author Contributions

All authors contributed to the study conception and design. Material preparation, data collection and analysis were performed. R.Y.M.: Methodology, writing-original draft preparation, and formal analysis. F.K.A.: Conceptualization, methodology, and formal analysis. A.F.A.: Methodology, writing-original draft preparation, visualization, and formal analysis. S.M.H.: Investigation, formal analysis, and reviewing and editing. S.M.A.: Conceptualization, methodology, and reviewing and editing. A.A.B. and M.A.A.: Investigation, formal analysis, and reviewing and editing. All authors have read and agreed to the published version of the manuscript.

Notes

The authors declare no competing financial interest.

ACKNOWLEDGMENTS

The authors would like to thank the University of Zakho, the University of Duhok, the Soran University, and the Salahaddin

University for their complete support. Also, the authors would like to thank the Soran research center at the Soran University for furnishing most of the facilities to complete this research study.

REFERENCES

(1) Martin, A., Harbison, S., Beach, K., Cole, P. *An Introduction To Radiation Protection*; Crc Press, 2018.
(2) Choi, T. A., Costes, S. V.; Abergel, R. J. Understanding The Health Impacts And Risks Of Exposure To Radiation. In *Reflections On The Fukushima Daiichi Nuclear Accident*; Springer: Cham, 2015.
(3) Vaiserman, A.; Koliada, A.; Zabuga, O.; Socol, Y. Health Impacts Of Low-Dose Ionizing Radiation: Current Scientific Debates And Regulatory Issues. *Dose-Response* **2018**, *16*, No. 155932581879633.
(4) Kim, J. H. Three principles for radiation safety: time, distance, and shielding. *Korean J. Pain* **2018**, *31*, 145−146.
(5) International Atomic Energy Agency, Radiation Safety of Gamma, Electron and X Ray Irradiation Facilities. In *IAEA Safety Standards Series No. SSG-8*; IAEA: Vienna, 2010.
(6) Al-Saadi, A. J.; Saadon, A. K. Gamma Ray Attenuation Coefficients for Lead Oxide and Iron Oxide Reinforced In Silicate Glasses as Radiation Shielding Windows. *Ibn AL-Haitham J. Pure Appl. Sci.* **2017**, *27*, 201−214. https://jih.uobaghdad.edu.iq/index.php/j/article/view/282
(7) Sayyed, M. I.; Akman, F.; Kaçal, M. R.; Kumar, A. Radiation protective qualities of some selected lead and bismuth salts in the wide gamma energy region. *Nucl. Eng. Technol.* **2019**, *51*, 860−866.
(8) Yoon, Y.; Truong, P. L.; Lee, D.; Ko, S. H. Phuoc Loc Truong, Daeho Lee, and Seung Hwan Ko, Metal-Oxide Nanomaterials Synthesis and Applications in Flexible and Wearable Sensors. *ACS Nanosci. Au* **2022**, *2*, 64−92.
(9) Yousefi, R.; Jamali-Sheini, F.; Cheraghizade, M.; Sa'aedi, A. Facile Synthesis And Optical Properties Of Pbo Nanostructures. *Lat. Am. Appl. Res.* **2014**, *44*, 163−166.
(10) Lipp, L.; Pletcher, D. The Preparation And Characterization Of Tin Dioxide Coated Titanium Electrodes. *Electrochim. Acta* **1997**, *42*, 1091−1099.
(11) Bratovcic, A. Synthesis, Characterization, Applications, and Toxicity of Lead Oxide Nanoparticles. In *Lead Chemistry*; IntechOpen, 2020, DOI: 10.5772/intechopen.91362.
(12) Chen, K.-C.; Wang, C.-W.; Lee, Y.-I.; Liu, H.-G. Nanoplates and nanostars of β-PbO formed at the air/water interface. *Colloids Surf., A* **2011**, *373*, 124−129.
(13) Asogwa, P. Band Gap Shift And Optical Characterization Of Pva-Capped Pbo Thin Films: Effect Of Thermal Annealing. *Chalcogenide Lett.* **2011**, *8*, 163−170.
(14) Ghasemi, S.; Mousavi, M.; Shamsipur, M.; Karami, H. Sonochemical-Assisted Synthesis Of Nano-Structured Lead Dioxide. *Ultrason. Sonochem.* **2008**, *15*, 448−455.
(15) Ahmed, S. M.; Mohammed, R. Y.; Abdulrahman, A. F.; Ahmed, F. K.; Hamad, S. M. Synthesis And Characterization Of Lead Oxide Nanostructures For Radiation Attenuation Application. *Mater. Sci. Semicond. Process.* **2021**, *130*, No. 105830.
(16) Yousefi, R.; Zak, A. K.; Jamali-Sheini, F.; Huang, N. M.; Basirun, W. J.; Sookhakian, M. Synthesis And Characterization Of Single Crystal Pbo Nanoparticles In A Gelatin Medium. *Ceram. Int.* **2014**, *40*, 11699−11703.
(17) Shi, L.; Xu, Y.; Li, Q. Controlled Growth Of Lead Oxide Nanosheets, Scrolled Nanotubes, And Nanorods. *Cryst. Growth Des.* **2008**, *8*, 3521−3525.
(18) Patnaik, P. *Handbook Of Inorganic Chemicals*; Mcgraw-Hill New York, 2003.
(19) Mousa, A. O.; Marmoss, A. F. Study The Structural And Electrical Properties Of Pbo Thin Films Deposited By Chemical Spray Pyrolysis Technique. *Int. J. ChemTech Res.* **2017**, *10*, 625−632.
(20) Ezugwu, S.; Asogwa, P.; Ezema, F.; Ejikeme, P. Structural And Optical Characterization Of Pvp-Capped Lead Oxide Nanocrystalline Thin Films. *J. Optoelectron. Adv. Mater.* **2010**, *12*, 1765.
(21) Mostaf, A. M. A.; Issa, S. A. M.; Zakaly, H. M. H.; Alotaibi, B. M.; Gharghar, F.; Al-Zaibani, M.; El Agammy, E. F. Radiation shielding and optical features for a PbO−BaO−B_2O_3 system. *Radiat. Phys. Chem.* **2023**, *202*, No. 110566.
(22) Uhm, Y. R.; Kim, J.; Lee, S.; Jeon, J.; Rhee, C. K. In Situ Fabrication Of Surface Modified Lead Monoxide Nanopowder And Its Hdpe Nanocomposite. *Ind. Eng. Chem. Res.* **2011**, *50*, 4478−4483.
(23) Nwodo, M.; Ezugwu, S.; Ezema, F.; Osuji, R.; Asogwa, P. Effect Of Thermal Annealing On The Optical And Structural, Properties Of Pbo Thin Film. *J. Optoelectron. Biomed. Mater.* **2011**, *3*, 95−100.
(24) Zhong, C.; Wang, X.; Wu, Y.; Li, L. Effect Of Pbo Seeding Layers On The Structure And Properties Of The Sol−Gel-Derived Bisco3−Pbtio3 Thin Films. *J. Am. Ceram. Soc.* **2010**, *93*, 3993−3996.
(25) Lokhande, R. M.; Vinayak, V.; Mukhamalec, S. V.; Khirade, P. P. Gamma radiation shielding characteristics of various spinel ferrite nanocrystals:a combined experimental and theoretical investigation. *RSC Adv.* **2021**, *11*, 7925.
(26) Tekin, H. O.; Sayyed, M. I.; Issa, S. A. M. Gamma radiation shielding properties of the hematite-serpentine concrete blended with WO_3 and Bi_2O_3 micro and nano particles using MCNPX code. *Radiat. Phys. Chem.* **2018**, *150*, 95−100.
(27) Pomaro, B. A Review on Radiation Damage in Concrete for Nuclear Facilities: From Experiments to Modeling. *Modell. Simul. Eng.* **2016**, *2016*, No. 4165746.
(28) Kaur, T.; Sharma, J.; Singh, T. Review on scope of metallic alloys in gamma rays shield designing. *Prog. Nucl. Energy* **2019**, *113*, 95−113.
(29) Kim, S.-C. Analysis of Shielding Performance of Radiation-Shielding Materials According to Particle Size and Clustering Effects. *Appl. Sci.* **2021**, *11*, 4010.
(30) Ezema, F.; Ekwealor, A.; Osuji, R. Optical Properties Of Chemical Bath Deposited Nickel Oxide (Niox) Thin Films. *J. Optoelectron. Adv. Mater.* **2008**, *21*, 6−10.
(31) Mohammed, R. Y. Annealing Effect On The Structure And Optical Properties Of Cbd-Zns Thin Films For Windscreen Coating. *Materials* **2021**, *14*, 6748.
(32) Zhang, L.; Guo, F.; Liu, X.; Cui, J.; Qian, Y. Metastable Pbo Crystal Grown Through Alcohol-Thermal Process. *J. Cryst. Growth* **2005**, *280*, 575−580.
(33) Kadhim, K. R.; Mohammed, R. Y. Effect of Annealing Time on Structure, Morphology, and Optical Properties of Nanostructured CdO Thin Films Prepared by CBD Technique. *Crystals* **2022**, *12*, 1315.
(34) Eid, G. A.; Kany, A.; El-Toony, M.; Bashter, I.; Gaber, F. Application Of Epoxy/Pb3o4 Composite For Gamma Ray Shielding. *Arab. J. Nucl. Sci. Appl.* **2013**, *46*, 226−233.
(35) Morris, V.; Farrell, R.; Sexton, A.; Morris, M. Lattice Constant Dependence On Particle Size For Ceria Prepared From A Citrate Sol-Gel. *J. Phys.: Conf. Ser.* **2006**, *26*, 119.
(36) Sundaresan, A.; Bhargavi, R.; Rangarajan, N.; Siddesh, U.; Rao, C. Ferromagnetism As A Universal Feature Of Nanoparticles Of The Otherwise Nonmagnetic Oxides. *Phys. Rev. B* **2006**, *74*, No. 161306.
(37) Kumar, S.; Kim, Y. J.; Koo, B.; Lee, C. G. Structural And Magnetic Properties Of Ni Doped Ceo2 Nanoparticles. *J. Nanosci. Nanotechnol.* **2010**, *10*, 7204−7207.
(38) Mythili, N.; Arulmozhi, K. Characterization Studies On The Chemically Synthesized A And B Phase Pbo Nanoparticles. *Int. J. Sci. Eng. Res.* **2014**, *5*, 412−416.
(39) Huse, V. R.; Mote, V. D.; Dole, B. N. The Crystallographic And Optical Studies On Cobalt Doped Cds Nanoparticles. *World J. Condens. Matter Phys.* **2013**, *3*, 46−49.
(40) Lizunova, A.; Mazharenko, A.; Masnaviev, B.; Khramov, E.; Efimov, A.; Ramanenka, A.; Shuklov, I.; Ivanov, V. Effects of Temperature on the Morphology and Optical Properties of Spark Discharge Germanium Nanoparticles. *Materials* **2020**, *13*, 4431.
(41) Elttayef, H. K.; Ajeel, H. M.; Kudair, A. E. Preparation And Study The Structural And Optical Properties Of Cus Nano Film. *Int. J. Thin Film Sci. Technol.* **2013**, *2*, 223.

(42) Droessler, L. M.; Assender, H. E.; Watt, A. A. Thermally Deposited Lead Oxides For Thin Film Photovoltaics. *Mater. Lett.* **2012**, *71*, 51−53.
(43) Abualroos, N. J.; Azman, M. N.; Amin, N. A. B.; Zainon, R. Tungsten-Based Material As Promising New Lead-Free Gamma Radiation Shielding Material In Nuclear Medicine. *Phys. Med.* **2020**, *78*, 48−57.
(44) Johnson, T. E. *Introduction To Health Physics*; Mcgraw Hill Education, 2017.
(45) Seenappa, L.; Manjunatha, H.; Chandrika, B.; Chikka, H. A Study Of Shielding Properties Of X-Ray And Gamma In Barium Compounds. *J. Radiat. Prot. Res.* **2017**, *42*, 26−32.
(46) Özdemir, T.; Güngör, A.; Akbay, I. K.; Uzun, H.; Babucçuoglu, Y. Nano Lead Oxide And Epdm Composite For Development Of Polymer Based Radiation Shielding Material: Gamma Irradiation & Attenuation Tests. *Radiat. Phys. Chem.* **2018**, *144*, 248.
(47) Gamal, R.; Salama, E.; Elshimy, H.; El-Nashar, D. E.; Bakry, A.; Ehab, M. Gamma Attenuation and Mechanical Characteristics of a Lead/NBR/SBR Rubber Composite with Black Nanocarbon Reinforcement. *Sustainability* **2023**, *15*, 2165.
(48) Aral, N.; Nergis, F. B.; Candan, C. Investigation Of X-Ray Attenuation And The Flex Resistance Properties Of Fabrics Coated With Tungsten And Barium Sulphate Additives. *J. Text. Apparel* **2016**, *26*, 166.
(49) Doğan, G. S. Lithium-Boro-Tellurite Glasses With Zno Additive: Exposure Buildup Factors (Ebf) And Nuclear Shielding Properties. *Avrupa Bilim Ve Teknoloji Dergisi* **2020**, 531−544.
(50) Tishkevich, D. I.; Grabchikov, S. S.; Lastovskii, S. B.; Trukhanov, S. V.; Zubar, T. I.; Vasin, D. S.; Trukhanov, A. V.; Kozlovskiy, A. L.; Zdorovets, M. M. Effect of the Synthesis Conditions and Microstructure for Highly Effective Electron Shields Production Based on Bi Coatings. *ACS Appl. Energy Mater.* **2018**, *1*, 1695−1702.
(51) Sallem, F. H.; Sayyed, M. I.; Aloraini, D. A.; Almuqrin, A. H.; Mahmoud, K. A. Characterization and Gamma-ray Shielding Performance of Calcinated and Ball-Milled Calcinated Bentonite Clay Nanoparticles. *Crystals* **2022**, *12*, 1178.
(52) AL-Rajhi, M. A.; Idriss, H.; Alaamer, A.-A. S.; El-Khayatt, A. M. Gamma/neutron radiation shielding, structural and physical characteristics of iron slag nanopowder, Applied Radiation and Isotopes. *Appl. Radiat. Isot.* **2021**, *170*, No. 109606.

https://doi.org/10.1021/acsomega.3c02910
ACS Omega 2023, 8, 22230−22237